Proteasome inhibition reduces proliferation, collagen expression, and inflammatory cytokine production in nasal mucosa and polyp fibroblasts

Laura Pujols, Laura Fernández-Bertolín, Mireya Fuentes-Prado, Isam Alobid, Jordi Roca-Ferrer, Neus Agell, Joaquim Mullol, César Picado

Clinical and Experimental Respiratory Immunoallergy, Institut d'Investigacions Biomèdiques August Pi i Sunyer (IDIBAPS) and Centro de Investigaciones Respiratorias en Red de Enfermedades Respiratorias (CIBERes), Barcelona, Spain (L.P., L.F-B, M.F.-P., I.A., J.R.-F., J.M., C.P); Unitat de Rinologia i clínica de l'olfacte, Servei d'Otorrinolaringologia, Hospital Clínic, Barcelona, Spain (I.A., J.M.); Departament de Biologia Cel·lular, Immunologia i Neurociències, Universitat de Barcelona, IDIBAPS, Barcelona, Spain (N.A.); Servei de Pneumologia i Al·lèrgia Respiratoria, Hospital Clínic, Universitat de Barcelona, Barcelona, Spain (C.P.).

Running title: proteasome inhibition in nasal fibroblasts

Correspondence to: Laura Pujols. Institut d'Investigacions Biomèdiques August Pi i Sunyer (IDIBAPS), lab 402. Hospital Clínic. Villarroel 170, 08036, Barcelona, Spain.

Fax: 34-934515272 / Tel: 34-932275400 (ext. 3282); e-mail: lpujols@clinic.ub.es

Number of text pages: 40 (from Abstract to Tables)

Number of tables: 1

Number of figures in the main manuscript: 8

Number of supplementary figures: 3

Number of references: 54

Number of words in the Abstract: 244

Number of words in the Introduction: 796

Number of words in the Discussion: 1,872

Abbreviations:

DMEM: Dulbecco's Modified Eagle's Medium

Erk1/2: extracellular signal regulated kinase1/2

FACS: fluorescence activated cell sorting

FBS: fetal bovine serum

csFBS: charcoal-stripped FBS

GM-CSF: granulocyte/macrophage colony-stimulating factor

IKK: IκB kinase

IL: interleukin

JNK: c-Jun-N-terminal kinase

MAPK: mitogen-activated protein kinase

MCP-1: monocyte chemoattractant protein-1

MKP-1: mitogen-activated protein kinase phosphatase-1

NF-κB: nuclear factor-κB

PARP: poly (ADP-ribose) polymerase

PBS: phosphate-buffered saline

PI3K/Akt: phosphoinositide 3-kinase/protein kinase B

PPAR-γ: peroxisome proliferator-activated receptor-γ

RANTES: regulated on activation normal T cell expressed and secreted

Rb: retinoblastomasiRNA: small interfering RNA

TNF-α: tumor necrosis factor-α

TGF-β: transforming growth factor-β

Recommended section assignment: Inflammation, Immunopharmacology, and Asthma

ABSTRACT

Proteasome inhibitors, used in cancer treatment for their pro-apoptotic effects, have anti-inflammatory and anti-fibrotic effects on animal models of various inflammatory and fibrotic diseases. Their effects in cells from patients affected by either inflammatory or fibrotic diseases have been poorly investigated. Nasal polyposis is a chronic inflammatory disease of the sinus mucosa characterized by tissue inflammation and remodeling. We tested the hypothesis that proteasome inhibition of nasal polyp fibroblasts might reduce their proliferation and their inflammatory and fibrotic response. Accordingly, we investigated the effect of the proteasome inhibitor MG262 on cell viability and proliferation, and on the production of collagen and inflammatory cytokines, in nasal polyp and nasal mucosa fibroblasts obtained from surgery specimens. MG262 reduced the viability of nasal mucosa and polyp fibroblasts concentration- and time-dependently, with marked effects after 48 h of treatment. The proteasome inhibitor bortezomib provoked a similar effect. MG262-induced cell death involved loss of mitochondrial membrane potential, caspase-3 and poly (ADP-ribose) polymerase activation, induction of c-Jun phosphorylation, and mitogen-activated protein kinase phosphatase-1 expression. Low concentrations of MG262 provoked growth arrest, inhibited DNA replication and retinoblastoma phosphorylation, and increased expression of the cell cycle inhibitors p21 and p27. MG262 concentration-dependently inhibited basal and TGF-β-induced collagen mRNA expression and IL-1β-induced production of IL-6, IL-8, MCP-1, RANTES and GM-CSF in both fibroblast types. MG262 inhibited IL-1β/TNF-α-induced activation of NF-κB. We conclude that non-cytotoxic treatment with MG262 reduces the proliferative, fibrotic, and inflammatory response of nasal fibroblasts, whereas high MG262 concentrations induce apoptosis.

INTRODUCTION

The ubiquitin-proteasome system is a multi-subunit enzyme complex present in the nucleus and cytoplasm of all eukaryotic cells; it plays a central role in the selective degradation of intracellular proteins that regulate transcription, cell cycle, apoptosis, cell adhesion, inflammatory processes and angiogenesis (Adams, 2003). An inhibitor targeting the proteasome, namely bortezomib, was approved by the FDA for the treatment of relapsed/refractory multiple myeloma (Wang et al., 2006; Meiners et al., 2008). Its efficacy relies on its capacity to induce the apoptosis of cells (preferentially transformed cells), through mechanisms involving inhibition of nuclear factor (NF)-κB and induction of the c-Jun-N-terminal kinase (JNK) pathway (Meiners et al., 2008). Owing to the key role of NF-κB in multiple inflammatory diseases, the use of proteasome inhibitors has been proposed as an anti-inflammatory strategy for treating non-neoplastic diseases (Wang et al., 2006; Meiners et al., 2008). They have been shown to reduce the inflammatory response in experimental animal models of hypertension (Ludwig et al., 2009), arthritis (Palombella et al., 1998; Yannaki et al., 2010), colitis (Schmidt et al., 2010), and asthma (Elliott et al., 1999). Proteasome inhibitors have also demonstrated anti-fibrotic effects on animal models of cardiac fibrosis (Meiners et al., 2004), muscle atrophy (Carmignac et al., 2011), and lung and skin fibrosis (Mutlu et al., 2012).

However, none of the numerous studies undertaken, both *in vitro* and *in vivo*, has clearly established the concentrations of the proteasome inhibitor that affect cell/animal viability and modulate cell function. In fact, the effect of proteasome inhibition on cell viability in non-cancerous cells has scarcely been investigated and has often been overlooked in studies reporting anti-inflammatory or anti-fibrotic effects of proteasome inhibitors. Furthermore, the anti-proliferative, anti-inflammatory and anti-fibrotic potential of proteasome inhibitors and their underlying mechanisms in the cells of patients affected by

either inflammatory or fibrotic diseases has been poorly investigated. These cells may significantly differ from cancerous cells in this respect.

Chronic rhinosinusitis with nasal polyps is a chronic inflammatory disease of the sinus mucosa characterized by both tissue inflammation and remodeling (Bachert et al., 2009). Nasal polyps reveal frequent epithelial damage, a thickened basement membrane, and an edematous stroma with abundant infiltration of inflammatory cells, predominantly activated eosinophils, and fibrotic foci. Nasal polyp fibroblasts are key producers of extra-cellular matrix proteins, such as collagens, as well as pro-inflammatory cytokines and chemokines.

In addition to maintaining the tissue structure, collagens are involved in cell adhesion, chemotaxis and migration in processes of growth, differentiation, and wound healing, and also in many pathological states. All collagens have three polypeptide chains, known as α-chains. There are at least 29 human collagen types, numbered from I to XXIX, which can be divided into several subfamilies on the basis of their supramolecular assemblies. Collagen types I, II and III, among others, are fibril-forming collagens (Myllyharju and Kivirikko, 2004). Collagen I, synthesized as two procollagen chains α1 and α2, each encoded by separate genes, is a major component of the extra-cellular matrix. An altered profile of collagens has been reported in the airways of asthmatics (Burgess, 2009). Patients with nasal polyps and associated asthma have increased fibroblast proliferation and extracellular matrix deposition, and increased fibroblast differentiation into myofibroblasts (Pawliczak et al., 2005). Collagens I and III are expressed by lung (Goulet et al., 2007) and nasal fibroblasts (Pujols et al., 2011), and their expression is induced by the pro-fibrotic stimulus transforming growth factor (TGF)-β.

Nasal polyp fibroblasts also release a variety of cytokines, chemokines and other pro-inflammatory mediators, including interleukin (IL)-6, IL-8, granulocyte/macrophage colony-stimulating factor (GM-CSF), monocyte chemoattractant protein (MCP)-1, and regulated on

activation normal T cell expressed and secreted (RANTES), that recruit and activate inflammatory cells into the nasal polyp site, thus contributing to the perpetuation of inflammatory and fibrotic processes in the tissue (Xing et al., 1993; Pujols et al., 2011).

Corticosteroids, the gold standard of nasal polyp treatment, are ineffective in some patients, who will require one or even several surgical operations to remove nasal polyps (Fokkens et al., 2007). Nasal polyps are, therefore, an optimal model for researching the etiology of chronic inflammatory airway diseases, as well as potential therapeutic treatments.

In the current work, we tested the hypothesis that proteasome inhibition of nasal polyp fibroblasts might reduce their proliferation and also modulate their inflammatory and fibrotic response. To do this, we used nasal fibroblasts obtained from both patients with nasal polyps and asthma and control subjects to characterize the effects of proteasome inhibition on the inflammatory and fibrotic cellular response. More specifically, we aimed to examine the effect of the proteasome inhibitor MG262 – which, like bortezomib, is a boronic peptide acid that selectively and reversibly inhibits the chymotryptic activity of the proteasome – on cell viability and proliferation, and on the production of collagen and inflammatory cytokines in nasal polyp and nasal mucosa fibroblasts.

MATERIALS AND METHODS

Reagents. Dulbecco's Modified Eagle's Medium (DMEM) was obtained from Lonza (Fisher Scientific, Pittsburgh, PA, USA) and fetal bovine serum (FBS) from Biological Industries (Kibbutz Beit Haemek, Israel). Trypsin-EDTA, penicillin, streptomycin, 4-(2-hydroxyethyl)-1-piperazineethanesulfonic acid (HEPES), small interfering RNA (siRNA) and all other transfection reagents were purchased from Invitrogen (Life Technologies; Carlsbad, CA, USA), and amphotericin B from Bristol-Myers Squibb (Middlesex, UK). MG262 [Z-Leu-Leu-Leu-B$(OH)_2$], IκB kinase (IKK) inhibitor III (BMS-345541), SP600125, SB203580, U0126, wortmannin, and caspase inhibitor I [Z-Val-Ala-Asp(OMe)-CH_2F, z-VAD-FMK] were obtained from Calbiochem (Merck Chemicals Ltd., Nottingham, UK), and bortezomib (Velcade) from Selleckchem (Houston, TX, USA). All drugs were dissolved in dimethylsulfoxide at least at 500 μM, and further diluted in cell culture medium. TGF-β, IL-1β and tumor necrosis factor (TNF)-α were purchased from R&D Systems (Abingdon, UK). Pifithrin-α [2-(2-imino-4,5,6,7-tetrahydrobenzothiazol-3-yl)-1-p-tolylethanone, HBr] and all other reagents were purchased from Sigma-Aldrich (St. Louis, MO, USA).

Subjects. Human nasal mucosa was obtained from 9 subjects (44.6 (mean) ± 4.6 (SEM) yr; 5 men) without any history of nasal or sinus disease who underwent nasal corrective surgery for turbinate hypertrophy or septal dismorphy. Nasal polyps were obtained from 12 patients (47.5 (mean) ± 3.1 (SEM) yr; 5 men) with diagnosis of nasal polyposis and asthma undergoing functional endoscopic sinus surgery. None of the patients had suffered from upper respiratory infection for at least 2 weeks prior to surgery. The diagnosis of nasal polyposis and asthma was based on established criteria, as reported elsewhere (Pujols et al., 2011). All the subjects agreed to participate in the study, which was approved by the Ethics Committee of our Institution.

Fibroblast culture. Fragments (approximately 3 x 3 mm) of the nasal tissues were placed in 6-well culture dishes in DMEM supplemented with 10% FBS, 100 U/ml penicillin, 100 μg/ml streptomycin, and 2 μg/ml amphotericin B, in a humidified atmosphere at 37ºC and 5% CO_2. Fibroblasts were isolated from the tissue fragments through adhesion and migration on the plastic surface, and further characterized by immunostaining of cytokeratin and vimentin, as previously reported (Pujols et al., 2011). In all the experiments, cells were growth-arrested by incubation with serum-free medium for 18 to 24 h prior to drug incubation. The experiments were carried out between passages 4 and 8.

Small interfering RNA silencing. Thirty to 50% confluent nasal fibroblasts were transfected with 20 nM of either c-Jun Silencer Select pre-designed siRNA (Part Number: 4392420) or Silencer Select negative control siRNA (Part Number: 4390843) duplexes in complex with lipofectamine RNAiMAX in OptiMem I (1.5 μl/well for 24-well plate, 7.5 μl/well for 6-well plate, or 15 μl/well for 6 cm dish). Medium was changed 18 h after transfection. Forty-eight hours after transfection, cells were incubated with MG262 (10 nM) for an additional 48 h.

Trypan blue exclusion assay. Fibroblasts were transfected and treated with MG262 as indicated above. The cell culture supernatants were collected and the trypan blue dye solution (0,4%) was added to the cell suspensions. The total number of dead cells was determined with standard hemocytometer procedure. Dead cells were seen as blue (permeable to dye due to disruption of the cell membrane).

Cell viability assays. Cells were plated in 96-well culture plates (1-2x10^3 cells/well). The following day, cells were growth-arrested as indicated above and incubated with cell medium supplemented with 0.5% FBS with/without the simultaneous addition of the proteasome inhibitor MG262 (0.1-1,000 nM) for 24, 48 and 72 h, or with the proteasome inhibitor bortezomib (0.1-1,000 nM) for 48 h. In some experiments, the caspase inhibitor z-VAD-FMK was added (50 μM) for 1 h prior to incubation with MG262. After treatment, cell viability was

determined using the colorimetric Cell Proliferation Kit II (XTT, Roche Diagnostics GmbH, Mannheim, Germany). This assay is based on the cleavage of the yellow tetrazolium salt XTT to form an orange formazan dye by metabolic active (viable) cells. Absorbance was measured on a microplate spectrophotometer at 490 nm.

Analysis of mitochondrial membrane potential (ΔΨm). Fibroblasts were incubated with cell medium supplemented with 0.5% FBS with/without the simultaneous addition of MG262 (50, 500 and 1,000 nM) for 24 h. After treatment, the cells were incubated with the fluorescent mitochondrial dye 3,3′-dihexyloxacarbocyanine iodide ($DiOC_6$, 40 nM) for 30 min at 37ºC. The cell culture supernatant was then collected and combined with the trypsinized (0.05% trypsin-0.02% EDTA) adherent cells. The cells were then centrifuged, resuspended in phosphate-buffered saline (PBS), and incubated for 15 min with a violet-fluorescent reactive dye (Live/Dead fixable dead cell stain kit, Invitrogen). The percentages of viable cells and those exhibiting loss of $DiOC_6$ uptake were finally determined by fluorescence activated cell sorting (FACS) with a FACSCantoII instrument (BD Biosciences, San Diego, CA, USA) and the data were analyzed using the FACSDiva software 6.1.2 (BD Biosciences).

Cell cycle analysis. Fibroblasts were treated with cell medium supplemented with 5% FBS with/without the simultaneous addition of MG262 (10 nM) for 24 h. The cells were then trypsinized, washed with PBS, fixed/permeabilized in 70% ethanol (overnight at 4ºC), washed again with PBS, and incubated for 30 min at 37ºC in a staining solution containing 0.34 mg/ml sodium citrate, 0.015 mg/ml propidium iodide and 0.3 mg/ml ribonuclease A. DNA content was then measured by FACS.

Analysis of DNA replication. Fibroblasts were treated with cell medium supplemented with 5% FBS with/without the simultaneous addition of MG262 (10 nM) for 22 h. Two hours before the end of treatment the non-radioactive thymidine nucleoside analogue 5-ethynyl-2´-

deoxyuridine (EdU) was added to the cell cultures. The cells were then trypsinized, washed with PBS, fixed in 70% ethanol (1 h, -20ºC), washed in 1% BSA in PBS, permeabilized with Triton X-100, and processed for the analysis of EdU incorporation into DNA, using the Click-iT EdU Flow cytometry Assay kit (Invitrogen) as indicated by the manufacturer.

Collagen mRNA expression. Fibroblasts were plated in six-well culture plates (10^5 cells/well) until sub-confluence, growth-arrested as indicated above and pre-incubated with cell medium without FBS and increasing concentrations of MG262 (1 to 50 nM) for 1 h. In some experiments, cells were incubated with 1 μM of the p53 inhibitor pifithrin-α in the absence or presence of MG262. TGF-β (5 ng/ml) was then added to the cell cultures and total RNA was extracted 24 h later using the RNeasy Mini kit (Qiagen). One microgram of total RNA was converted to cDNA using the High-Capacity cDNA Reverse Transcription Kit (Applied Biosystems). The mRNA expression of collagens 1α1, 1α2, 3α1, and RNA polymerase II was analyzed by real-time PCR (7900HT Fast Real-Time PCR System, Applied Biosystems) using TaqMan Fast Universal PCR Master Mix and TaqMan Gene Expression Assays (Assay ID's: Hs00164004_m1, Hs00164099_m1, Hs00164103_m1, Hs00172187_m1, Applied Biosystems). Collagen mRNA expression was normalized to the mRNA expression of the constitutive gene RNA polymerase II, as published elsewhere (Pfaffl et al., 2001).

Cytokine production. Fibroblasts were plated in 24-well culture plates ($3x10^4$ cells/well) until sub-confluence, growth-arrested as indicated above and pre-incubated with cell medium supplemented with 10% charcoal-stripped FBS (csFBS, Invitrogen) in the absence or presence of increasing concentrations of MG262 (5 to 500 nM) for 1 h. In some experiments, cells were pre-incubated (1 h) with the IKK/NF-κB inhibitor BMS-345541 (10 μM), the JNK mitogen-activated protein kinase (MAPK) inhibitor SP600125 (20 μM), the p38 MAPK inhibitor SB203580 (10 μM), the MAPK kinase MEK1/2 inhibitor U0126 (10 μM), and the

phosphoinositide 3-kinase/protein kinase B (PI3K/Akt) inhibitor wortmannin (1 μM). Cells were then stimulated with 10 ng/ml of IL-1β or TNF-α (R&D Systems) for 4 h. IL-6 and IL-8 production in supernatants was measured by ELISA (DuoSet ELISA, R&D Systems). MCP-1, RANTES, and GM-CSF production in supernatants was measured using specific BD Cytometric Bead Array (CBA) Flex Sets (BD Biosciences) by FACS, following the recommendations of the manufacturer. Cytokine production (pg/ml) was corrected by cell number using the XTT assay.

Western blot. Cells were lysed in a lysis buffer containing 50 mM Tris-HCl (pH 7.4), 150 mM NaCl, 0.1% sodium dodecyl sulfate (SDS), 1% NP-40 Igepal, 1 μg/ml leupeptin, 1 μg/ml aprotinin, 0.1 mM Na_3VO_4, 1 mM NaF, 1 mM dithiothreitol, 0.5 mg/ml Pefabloc, and 5 mg/ml sodium deoxycholate. Cell extracts (20-30 μg) were electrophoresed in SDS-polyacrylamide gels and transferred to nitrocellulose membranes. Membranes were pre-incubated for 1 h at room temperature in T-TBS (10 mM Tris-HCl [pH 7.4], 150 mM NaCl, 0.1% Tween 20) containing either 5% fat-free powdered milk or 5% BSA, and then incubated (overnight at 4ºC) with the primary antibodies against p27 (cat. # sc-528), total retinoblastoma (Rb, cat. # sc-102), cyclin D1 (cat. # sc-20044), total (cat. # sc-45) and phosphorylated (Ser63, cat. # sc-822) c-Jun, MAPK phosphatase (MKP)-1 (cat. # sc-370), peroxisome proliferator-activated receptor-γ (PPAR-γ, cat. # sc-7196) (Santa Cruz Biotechnology, Santa Cruz, CA, USA), p53 (Ab-5, cat. # MS-186, Thermo Scientific, Cheshire, UK), phosphorylated (Ser807/811) Rb (cat. # 9308), phosphorylated (Thr180/Tyr182) p38 MAPK (cat. # 9215), cleaved caspase-3 (cat. # 9661), cleaved poly (ADP-ribose) polymerase (PARP, cat. # 9546) (Cell Signaling, Beverly, MA, USA), p21 (Cat. # OP64), phosphorylated (Ser32) IκB-α (cat. # 400002, Calbiochem), and β-actin (cat. # A5441, Sigma). After washing with T-TBS, the membranes were incubated with the appropriate peroxidase-conjugated secondary antibodies for 1 h at room temperature, washed, and finally visualized by enhanced

chemiluminescence reaction (SuperSignal West Pico, Invitrogen). Light emission was detected by a CCD camera (LAS-3000, Fujifilm).

Immunocytochemistry. Fibroblasts were treated with cell medium supplemented with 10% csFBS in the absence or presence of 500 nM MG262 for 1 h, and then stimulated with TNF-α or IL-1β (100 ng/ml each) for 30 min. The cells were then fixed in 4% paraformaldehyde, permeabilized in 0.1% Triton X-100 - 1% BSA, incubated with anti-p65 antibody (Cat. # sc-372, Santa Cruz), washed in PBS, incubated with secondary antibody conjugated to Alexa 488, mounted in Prolong® Gold aqueous mounting medium (Molecular Probes) and visualized by fluorescence microscopy (DMI6000B, Leica Microsystems, Wetzlar, Germany). Photographs were taken with a Leica DF350 FX digital camera and processed using the LAS AF software (Leica).

Statistical analysis. Results are expressed as median and 25th to 75th percentiles. Multiple comparisons, such as concentration-response experiments, were analyzed using one-way ANOVA with Tukey/Dunnett post hoc analysis if variables were normally distributed and had similar variances, the latter calculated using the Barlett's test or the Levene's test. If the variable distributions were not normal and/or had different variances, the Kruskal-Wallis with Dunn's post hoc analysis was used instead. Similarly, comparisons between two groups were made with the t-test if data were normally distributed and had similar variances or the Mann-Whitney U test if the variable distributions were not normal and/or had different variances. The concentration (nM) of drug that results in 50% inhibition (IC_{50}) of the effect provoked by the stimulus was calculated with the GraphPad Prism software. Statistical analyses were performed with SPSS and GraphPad Prism software. Statistical significance was established as $p < 0.05$.

RESULTS

Effect of MG262 on fibroblast viability. It is well known that the efficacy of proteasome inhibitors, in particular bortezomib, in cancer relies on their capacity to induce cell death (Meiners et al., 2008). However, the effect of proteasome inhibitors on cell viability in non-cancerous cells has been less widely investigated and remains controversial (Fineschi et al., 2006; You and Park, 2011). In an attempt to discern the concentration and incubation time with the proteasome inhibitor MG262 that affect the viability of nasal fibroblasts, we carried out concentration-response and time-course experiments with the proteasome inhibitor MG262 and analyzed the viability of nasal fibroblasts thereafter by using the XTT metabolic assay. As shown in Figure 1A, the treatment of nasal fibroblasts with MG262 for 24 h provoked a significant concentration-dependent reduction in cell viability in both nasal mucosa and nasal polyp fibroblasts. The maximal suppression reached approximately 40% in both cases. A marked concentration-dependent decrease in cell viability was found after 48 h (Figure 1B) and 72 h (Figure 1C) of MG262 treatment. No differences in IC_{50} (median, nM; 25^{th}-75^{th} percentiles) were found between nasal mucosa (48 h: 11; 10-23; 72 h: 4; 3-6) and nasal polyp fibroblasts (48 h: 7; 5-35; 72 h: 4; 3-8; ns). A significant decrease in cell viability was also found after 48 h of fibroblast treatment with the proteasome inhibitor bortezomib (Figure 1D). IC_{50} values for bortezomib did not either differ between nasal mucosa (36; 10-191) and polyp fibroblasts (24; 17-67; ns).

Effect of MG262 on apoptosis. Because we found that MG262 reduced the viability of nasal fibroblasts and proteasome inhibitors are known to provoke tumor cell death via the induction of apoptosis (Hideshima et al, 2001), we reasoned that the cell death of nasal fibroblasts provoked by MG262 would also involve apoptosis. The initial apoptotic pathways end at the point of the execution phase, considered the final pathway of apoptosis, where the activation of executioner caspases (of which caspase-3 is the most important) provokes the cleavage of

various substrates, such as poly (ADP-ribose) polymerase (PARP), that ultimately cause the morphological and biochemical changes seen in apoptotic cells (Elmore, 2007). To elucidate whether MG262 induced nasal fibroblast apoptosis, fibroblasts were either pre-incubated with the caspase inhibitor z-VAD-FMK (50 μM) prior to incubation with MG262 or were not treated, and cell viability was analyzed by the XTT assay. As shown previously, incubation with high concentrations of MG262 for 48 h significantly reduced fibroblast viability compared to non-treated cells (Figure 2A). More importantly, z-VAD-FMK partially prevented the reduction of fibroblast viability provoked by MG262, suggesting that the decrease in cell viability provoked by long-term exposure with MG262 involves apoptosis.

The loss of mitochondrial membrane potential is one of the earliest events that initiates the classical intrinsic pathway of apoptosis (Elmore, 2007) and proteasome inhibitors are known to induce this event in cancer cells (Ling et al., 2003b; Domingo-Domènech et al., 2008). We therefore aimed to investigate whether MG262 provoked the loss of mitochondrial membrane potential in nasal fibroblasts. As shown in Figure 2B, incubation of fibroblasts with MG262 for 24 h caused a significant concentration-dependent loss of mitochondrial membrane potential. We then explored whether MG262 provoked the activation of caspase-3 and that of its substrate PARP in nasal fibroblasts, as occurs after proteasome inhibition of tumor cells (Hideshima et al., 2001; Ling et al., 2003a; Ling et al., 2003b). Treatment with 50 nM MG262 for 24 h did not result in the expression of cleaved caspase-3, or its substrate PARP, in any fibroblast line (Figure 2C). At 24 h, expression of cleaved caspase-3 was only found at the highest concentration of MG262 (1,000 nM). Expression of cleaved caspase-3 and PARP was detected after cell incubation with 50 nM MG262 for 48 h (Figure 2C).

Induction of the JNK MAPK stress pathway is another reported mechanism by which proteasome inhibitors provoke apoptosis of tumor cells (Meiners et al., 2008; Hideshima et al., 2003; Yang et al., 2004). The activity of JNK and other MAPK is endogenously

controlled by different MAPK phosphatases, such as MKP-1 (Liu et al., 2007). MKP-1 is degraded through the proteasome and is known to be activated by proteasome inhibitors in cancer cells (Small et al., 2004). We hypothesized that MG262 would also activate the JNK pathway and MKP-1 in nasal fibroblasts. Accordingly, treatment of nasal fibroblasts with MG262 (50 nM) markedly induced c-Jun phosphorylation 6 and 24 h after administration (Figures 3A and 3B, upper graph), and also induced MKP-1 expression (Figures 3A and 3B, lower graph). We then examined the involvement of c-Jun activation on the pro-apoptotic effect of MG262 on our cells by silencing c-Jun expression using small interfering RNA (siRNA) techniques. We first demonstrated that MG262-induced c-Jun phosphorylation was abrogated in c-Jun siRNA-transfected cells (Figure 3C). Interestingly, the induction of cell death provoked by the exposure of nasal fibroblasts to 10 nM MG262 for 48 h was significantly abrogated in c-Jun siRNA-transfected cells (Figure 3D and 3E), which indicates that the increase in cell death provoked by long-term exposure with MG262 involves activation of the JNK/c-Jun pathway.

Effect of MG262 on the cell cycle. Exposure of cancer cells to proteasome inhibitors causes cell-cycle arrest (Codony-Servat et al., 2006; Ling et al., 2003a; Domingo-Domènech et al., 2008). We investigated whether MG262 also caused cell-cycle arrest in nasal fibroblasts. As expected, the treatment of growth-arrested fibroblasts with a cell growth stimulus, i.e. 5% FBS, markedly increased the S phase and G2/M population and, consequently, decreased the G0/G1 population (Figure 4A and Table 1). MG262 (10 nM), added simultaneously to the stimulus, provoked the complete arrest of cell cycle progress compared to 5% FBS-treated cells. Thus, MG262-treated cells had a percentage of cells in G0/G1, S and G2/M similar to that of FBS-deprived cells, indicating that MG262 did not allow cells to progress into the S phase. At this concentration, MG262 did not significantly increase the sub-G0/G1 population associated with cell death, compared to both FBS-deprived and 5% FBS-treated cells (Figure

4A). MG262 caused cell accumulation at S and G2/M in asynchronized (non-growth-arrested) cell cultures (data not shown). Confirming the propidium iodide staining findings (Figure 4A), MG262 (10 nM) completely abolished cell proliferation (DNA replication), the percentage of proliferating cells being similar to that of FBS-deprived cells (Figure 4B and Table 1).

Progression through the G1 cell-cycle restriction point is controlled by the phosphorylation status of retinoblastoma (Rb). Rb phosphorylation induced by cyclin-cyclin-dependent kinase (CDK) complexes (cyclin D-CDK4/6 first, followed by cyclin E-CDK2) provokes Rb inactivation, thus permitting the release of the transcription factor E2F and cell-cycle progression (Poznic et al., 2009). CDK activity is negatively regulated by CDK inhibitors, including p21 and p27 (Sherr et al., 1999). Since we found that MG262 provoked a cell-cycle arrest of nasal fibroblasts that did not allow cells to progress into the S phase, we hypothesized that some of the cell-cycle proteins that regulate the G1-S transition might be affected by MG262. As expected, the incubation of nasal fibroblasts with 5% FBS for 6 h, and more particularly for 24 h, provoked hyperphosphorylation of Rb compared to serum-deprived cells (Figures 5A and 5B). MG262 treatment, even at the lowest concentration tested (5 nM), completely inhibited Rb phosphorylation, in keeping with the findings of the blockade of cell cycle progression by MG262 (Figure 4). In addition, the incubation of fibroblasts with 5% FBS for 6 h significantly increased the expression of the positive regulatory cell-cycle protein cyclin D1, and MG262 increased (without statistical significance) cyclin D1 expression, compared to FBS-treated cells (Figure 5C). MG262 also provoked a time- and concentration-dependent increase in the expression of the cell-cycle inhibitors p21, and to a lesser extent that of the p27 (Figures 5D and 5E).

Effect of MG262 on collagen mRNA expression. Once the effect of MG262 on the cell cycle and viability of nasal fibroblasts had been characterized, we aimed to determine the

capacity of MG262 to modulate, and more specifically to decrease, their fibrotic and inflammatory response. One of the first studies assessing the anti-fibrotic potential of proteasome inhibitors reported a decrease in collagen mRNA expression after proteasome inhibition of human dermal fibroblasts (Fineschi et al., 2006). We therefore investigated whether MG262 also reduced collagen expression in nasal fibroblasts. In agreement with our previous studies (Pujols et al., 2011), the pro-fibrogenic stimulus TGF-β (5 ng/ml) induced the mRNA expression of collagens 1α1, 1α2 and 3α1 in both nasal mucosa and polyp fibroblasts (Figure 6A). No significant differences were found between nasal mucosa and polyp fibroblasts as regards the extent of mRNA induction by TGF-β of the three collagen types. MG262 provoked a concentration-dependent decrease in the TGF-β-induced mRNA expression of the three collagen types in both nasal mucosa and polyp fibroblasts (Figure 6A). At 50 nM, MG262 inhibited the mRNA expression of all three collagens more than the basal condition (no TGF-β). Indeed, as shown in Figure 6B, MG262 also markedly suppressed the basal expression of collagens.

We then attempted to elucidate the mechanisms by which MG262 suppressed collagen mRNA expression in nasal fibroblasts. We have already demonstrated that MG262 increased c-Jun phosphorylation induced by 5% FBS (Figure 3A and 3B). Previous reports have shown that stimulation of the JNK/activator protein (AP)-1 pathway by phorbol 12-myristate 13-acetate or estradiol leads to the suppression of type I collagen synthesis (Silbiger et al., 1999). Based on these observations, we hypothesized that MG262 would also increase c-Jun phosphorylation induced by TGF-β, and that such an increase might partly explain the suppressive effect of MG262 on collagen expression in our cells. As shown in Figure 6C, MG262 markedly increased c-Jun phosphorylation in both basal and TGF-β-stimulated nasal fibroblasts. To elucidate whether this induced c-Jun phosphorylation was involved in the suppression of collagen expression by MG262, we analyzed the effect of MG262 in cells with

a silenced expression of c-Jun. The suppression of TGF-β-stimulated collagen mRNA expression by MG262 was not abrogated, however, in c-Jun siRNA-transfected nasal fibroblasts (data not shown).

The gene expression of type I collagen induced by TGF-β is primarily mediated via the Smad signaling pathway, where, after phosphorylation by the activated type I TGF-β receptor, cytoplasmic Smad2 and Smad3 heterodimerize with Smad4 and accumulate within the nucleus, where they recruit cofactors to Smad-binding elements in the collagen gene promoter and thereby activate collagen transcription (Ghosh, 2002). One of the numerous proteins found to repress TGF-β-induced collagen gene expression is the nuclear hormone receptor PPAR-γ (Ghosh et al., 2009). It has recently been reported that bortezomib inhibits TGF-β-mediated target gene expression in lung fibroblasts, partly by increasing PPAR-γ abundance and activity (Mutlu et al., 2012). We expected that MG262 would similarly increase PPAR-γ protein levels in nasal fibroblasts but it failed to do so in both basal and TGF-β-stimulated nasal fibroblasts (Figure 6C).

The tumor suppressor p53 has also been reported as a potent repressor of TGF-β-regulated collagen gene expression in fibroblasts (Ghosh et al., 2004; Nacu et al., 2008). Proteasome inhibitors are known to up-regulate the expression of p53 in multiple myeloma cells (Hideshima et al., 2003). We therefore hypothesized that MG262 would increase p53 levels in nasal fibroblasts, and that such an increase may partly explain the suppressive effect of MG262 on collagen expression. As shown in Figure 6C, MG262 increased p53 levels in both basal and TGF-β-stimulated nasal fibroblasts. To elucidate whether this increase in p53 was involved in the suppression of collagen expression by MG262, we analyzed the capacity of MG262 to suppress collagen mRNA expression in cells whose p53 activity was inhibited by cell treatment with 1 μM of the p53 inhibitor pifithrin-α. MG262 still markedly inhibited

both basal and TGF-β-stimulated collagen mRNA expression in pifithrin-α-treated fibroblasts (supplementary Figure 1).

Effect of MG262 on the production of pro-inflammatory cytokines. In order to determine the anti-inflammatory potential of proteasome inhibition in nasal fibroblasts, we first investigated the effect of MG262 on the production of the pro-inflammatory cytokines IL-6 and IL-8, which are released in high amounts by these cells (Pujols et al., 2011). As expected, the treatment of cells with 10 ng/ml of the pro-inflammatory stimuli IL-1β (Figure 7A) or TNF-α (supplementary Figure 2) for 4 h markedly induced IL-6 and IL-8 production in both nasal mucosa and polyp fibroblasts, compared to non-stimulated cells. MG262 concentration-dependently inhibited IL-1β-induced IL-6 and IL-8 production in both fibroblast types (Figure 7A). MG262 also inhibited TNF-α-induced IL-6 and IL-8 production in both fibroblast types, although inhibition did not reach statistical significance for IL-6 (supplementary Figure 2). Under the conditions tested in this study, MG262 did not significantly alter cell viability, as determined by the XTT assay, compared to non-MG262-treated cells (data not shown).

We then aimed to elucidate the mechanisms by which MG262 could inhibit IL-1β-induced IL-6 and IL-8 release in nasal fibroblasts. The main proposed mechanism by which proteasome inhibitors reduce the release of a variety of pro-inflammatory mediators is through inhibition of NF-κB (Meiners et al, 2008). Nevertheless, we first determined the intracellular signaling pathways involved in IL-1β-induced IL-6 and IL-8 release. The release of IL-6 and IL-8 induced by IL-1β was completely abrogated by the pre-treatment of nasal fibroblasts with the IKK/NF-κB inhibitor BMS-345541, and inhibited to a lesser extent by the p38 and JNK MAPK inhibitors SB203580 and SP600125, respectively (Figure 7B). Consequently, we first explored whether cytokine inhibition by MG262 involved reduced NF-κB activation. MG262 prevented the translocation of the NF-κB subunit p65 to the cell nucleus induced by both IL-1β (Figure 7C) and TNF-α (supplementary Figure 3), and also

prevented the degradation of p-IκBα in IL-1β-stimulated fibroblasts (Figure 7D). In addition, treatment of cells with MG262, under the same experimental conditions that inhibited IL-6 and IL-8 release (Figure 7A), increased the phosphorylation of p38 and c-Jun MAPK in both basal and IL-1β-stimulated fibroblasts (Figure 7E). Therefore, the inhibitory effect of MG262 on cytokine release does not occur through inhibition of either c-Jun or p38 MAPK.

Finally, we determined whether the inhibitory effects of MG262 on IL-6 and IL-8 production also occurred for other pro-inflammatory cytokines and chemokines, more specifically MCP-1, RANTES and GM-CSF. These molecules are secreted by nasal fibroblasts upon exposure to different proinflammatory or stressful stimuli and they are known to participate in the recruitment and activation of monocytes, lymphocytes, or eosinophils to the inflammatory site (nasal polyp) (Xing et al., 1993; Meyer et al., 1998; Nonaka et al., 1999; Le Bellego et al., 2009). MG262 provoked a significant concentration-dependent decrease in the IL-1β-induced production of MCP-1, RANTES and GM-CSF in nasal mucosa and polyp fibroblasts (Figure 8).

DISCUSSION

This is the first study to assess the effect of proteasome inhibition on the proliferation and regulation of the cell's function in primary airway fibroblasts – in this case nasal fibroblasts – from both control subjects and patients with airway inflammatory diseases (in this case nasal polyposis and asthma).

Using the XTT assay, we first found that MG262 reduced the viability of nasal fibroblasts, especially after 48 and 72 h of treatment. Cell viability was similarly reduced by the exposure of nasal fibroblasts to bortezomib. Proteasome blockade was as effective in nasal polyp as in control nasal mucosa fibroblasts. The kinetics and sensitivity (IC_{50}) of MG262 and bortezomib inhibition was similar to those reported for bortezomib in cancer cell lines (Hideshima et al., 2001; Codony-Servat et al., 2006). Our results concur with those reported in human pulmonary fibroblasts using the proteasome inhibitor MG132 (You and Park, 2011) and in bortezomib-treated rat fibroblast-like synoviocytes (Yannaki et al., 2010), but contrast with those of Fineschi and coworkers (Fineschi et al., 2006 and 2008). The latter, using a similar experimental approach and analytical method, found that MG262 and proteasome inhibitor I decreased the viability of human dermal fibroblasts only when used at very high (micromolar) concentrations after 72 h of culture (Fineschi et al., 2006). This suggests that the sensitivity to MG262-induced cell death would depend on the fibroblast origin, i.e., nose *versus* skin. These authors then reported that exposure of murine lung fibroblasts to 1 μM bortezomib for 24 h similarly had no effect on cell viability (Fineschi et al., 2008), which contrasts with the inhibitory effect of MG262 on nasal fibroblast viability when used at an equivalent time and concentration.

MG262 provoked the loss of mitochondrial membrane potential in nasal fibroblasts, thus confirming that the decrease in cell viability by MG262 was due to the induction of apoptosis. The induction of this early apoptotic event by proteasome inhibitors has been

reported in cancer cells (Ling et al., 2003b; Domingo-Domènech et al., 2008) and also in human pulmonary fibroblasts (You and Park, 2011). Our results using the caspase inhibitor z-VAD-FMK revealed that the decrease in nasal fibroblast viability provoked by MG262 involved caspase-mediated apoptosis. Accordingly, and in agreement with studies in cancerous (Hideshima et al., 2001; Ling et al., 2003a; Ling et al., 2003b) and non-cancerous cells (Kawakami et al., 1999; Goldbaum et al., 2006), MG262 induced the activation of the apoptotic enzymes caspase-3 and PARP in nasal fibroblasts. However, compared to cancer cell lines, these enzymes appear to be much less activated by proteasome inhibition in our cells, thus requiring very high concentrations of MG262 (1,000 nM) for at least 24 h to be detected. This may be because nasal fibroblasts are more resistant to proteasome inhibitor-mediated apoptosis than other cell types, or because proteasome inhibitor-mediated apoptosis in our cells primarily involves apoptotic mediators other than caspase-3 and PARP.

In line with studies reported in tumor cells (Hideshima et al., 2003; Yang et al., 2004), MG262 provoked a strong activation (phosphorylation) of c-Jun in nasal fibroblasts. The involvement of c-Jun activation in MG262-induced cell death was further demonstrated in transfection experiments with c-Jun siRNA. MG262 also activated MKP-1 expression in our cells. The induction of MKP-1 by proteasome inhibitors is reported to play an anti-apoptotic role through down-regulation of JNK activity (Small et al., 2004). Effectively, the over-expression of MKP-1 in cancer is reported to be a bad prognostic factor for curing the disease (Small et al., 2007). In our fibroblasts, MG262-induced MKP-1 expression does not appear to down-regulate c-Jun activity, as the phosphorylation of c-Jun was strongly induced by MG262, but a possible relationship between these two events has not been investigated. Conversely, the current study has not explored whether inhibition of MKP-1 would further enhance the JNK pathway and, as a result, increase the apoptotic capacity of MG262.

Proteasome inhibitors cause cell-cycle arrest, particularly a G2/M arrest, in cancer cells (Codony-Servat et al., 2006; Ling et al., 2003a; Domingo-Domènech et al., 2008). The use of synchronized (growth-arrested) cultures showed that this arrest takes place not only in G2/M but also in G0, G1 or G1/S transition in nasal fibroblasts. In keeping with the blocking effects of MG262 on the cell cycle, MG262 inhibited the proliferation (DNA replication) of nasal fibroblasts. These results concur with the marked inhibition of cell proliferation after the incubation of fibroblast-like synoviocytes with bortezomib, at the same concentration (10 nM) used in our study (Yannaki et al., 2010).

MG262 inhibited Rb phosphorylation and, in agreement with data reported in cancerous cells (Hideshima et al., 2001; Ling et al., 2003a; Codony-Servat et al., 2006), increased the expression of p21 and p27 in nasal fibroblasts. Since p21 and p27 are well-known proteasome substrates (Adams et al., 2003), their increase by MG262 is most probably the result of their inhibited degradation. The increase in cyclin D1 levels after fibroblast treatment with MG262 is unsurprising because cyclin D1 is also degraded by the proteasome (Guo et al., 2005). Therefore, the lack of Rb phosphorylation, and consequently the inhibition of cell-cycle progression, provoked by MG262 in nasal fibroblasts must be the consequence of increased p21 and p27 rather than any lack of cyclin D1.

We have explored the capacity of MG262 to down-regulate the pro-fibrotic function of nasal fibroblasts. We previously reported that TGF-β induced the mRNA expression of collagen types 1α1, 1α2 and 3α1 in nasal fibroblasts – an induction not abrogated by glucocorticoid treatment (Pujols et al., 2011). We now report that moderately low concentrations of MG262 (10-50 nM) significantly reduce the mRNA expression of the three collagen types in both unstimulated and TGF-β-stimulated nasal mucosa and polyp fibroblasts. Similarly, a decrease in collagen mRNA expression has been reported after proteasome inhibition of human dermal (Fineschi et al., 2006; Goffin et al., 2010) and murine

lung fibroblasts (Fineschi et al., 2008). Proteasome inhibition in rat cardiac fibroblasts also decreased collagen mRNA expression and expression of matrix metalloproteinases 2 and 9 (Meiners et al., 2004). It has recently been reported that bortezomib inhibits TGF-β-mediated target gene expression in human lung fibroblasts from normal individuals and patients with idiopathic pulmonary fibrosis, and in skin fibroblasts from a patient with scleroderma (Mutlu et al., 2012).

The mechanisms by which proteasome inhibitors suppress collagen expression have not been fully elucidated. Numerous transcription factors and cofactors are known to be involved in the regulation of both basal and TGF-β-stimulated type I collagen gene expression, including, among others, SP1, AP-1, different Smad family members, CBP/p300, PPAR-γ, and p53 (Ghosh, 2002; Ghosh et al., 2009). As opposed to results reported in lung fibroblasts (Mutlu et al., 2012), PPAR-γ levels were not increased by exposure of nasal fibroblasts to MG262. We found that MG262 increased c-Jun phosphorylation and p53 levels in both unstimulated and TGF-β-stimulated nasal fibroblasts, but none of these effects could explain the marked suppressive effect of MG262 on collagen expression. With regard to other transcription factors involved in TGF-β-induced collagen expression, Goffin and coworkers (2010) reported that bortezomib did not affect TGF-β-induced Smad2 phosphorylation, nuclear translocation, or binding to the collagen 1α2 promoter. In fact, Fineschi and coworkers (2008) reported an increase in TGF-β-induced Smad2 phosphorylation by proteasome inhibitors. Mutlu and coworkers (2012) similarly found that bortezomib did not inhibit TGF-β-induced Smad3 phosphorylation or nuclear translocation, although it inhibited the transcription of a Smad-responsive luciferase reporter construct. It is worth noting that bortezomib abrogated the binding of SP1 to the collagen 1α2 promoter in both untreated and TGF-β-stimulated fibroblasts (Goffin et al., 2010). Analysis of the possible role of SP1 will be the subject of future experiments but are beyond the scope of the current manuscript.

We have also explored the capacity of MG262 to regulate the production of pro-inflammatory cytokines and chemokines by nasal fibroblasts. MG262 reduced the IL-1β- and TNFα-induced release of IL-6 and IL-8 by both nasal mucosa and polyp fibroblasts. In agreement with our results, a decrease in IL-6 production has been reported after proteasome inhibition of TNF-α-stimulated airway smooth muscle cells (Moutzouris et al., 2010), LPS plus phorbol 12-myristate 13-acetate-stimulated U937 monocytes (Ortiz-Lazareno et al., 2008), and multiple myeloma cell lines (Hideshima et al., 2001). Controversial results have been obtained with regard to IL-8: in line with our results, proteasome inhibition of LPS-stimulated macrophages has led to decreased IL-8 levels (Cuschieri et al., 2004), but increased IL-8 levels have also been reported after the proteasome inhibition of various cell types (Hipp et al., 2002; Gerber et al., 2004). MG262 also decreased the IL-1β-induced production of other pro-inflammatory mediators, i.e., MCP-1, RANTES and GM-CSF, known to participate in the recruitment and activation of inflammatory cells on the nasal polyp site (Xing et al., 1993; Meyer et al., 1998; Nonaka et al., 1999; Le Bellego et al., 2009). The inhibition of one or more of these mediators by proteasome inhibitors has also been reported in human airway smooth muscle (Moutzouris et al., 2010) and endothelial cells (Hipp et al., 2002).

The potent anti-inflammatory effects of proteasome inhibitors have been mainly attributed to attenuated activation of the pro-inflammatory transcription factor NF-κB (Meiners et al, 2008). Our experiments using intracellular pathway-specific inhibitors revealed that activation of NF-κB is critical in the induction of IL-6 and IL-8 production by IL-1β in nasal fibroblasts. Although we did not directly demonstrate this, NF-κB is also likely to be critical in the induction of MCP-1, RANTES and GM-CSF by IL-1β in nasal fibroblasts, since the expression of these genes is also regulated by NF-κB (Barnes and Karin, 1997). Interestingly, and in line with previous studies (Palombella et al., 1998; Codony-Servat et al.,

2006), MG262 blocked the IL-1β-stimulated activation of NF-κB in nasal fibroblasts via two distinct mechanisms: firstly by preventing the degradation of the NF-κB inhibitor IκBα, and secondly by impairing IL-1β/TNF-α-induced translocation of NF-κB to the cell nucleus.

In summary, our study shows that the proteasome inhibitor MG262, when administered at high concentrations or for long exposure times, provokes the cell death of primary nasal mucosa and polyp fibroblasts via the induction of apoptosis, by involving the expression of cleaved caspase-3 and PARP, and phosphorylation of c-Jun. Lower concentrations of MG262 block the progression of the cell cycle, by involving the inhibition of Rb phosphorylation and an increase in the cell-cycle inhibitors p21 and p27. MG262 inhibits the functional activity of nasal fibroblasts by reducing both basal and TGF-β-induced expression of collagens and also by down-regulating the production of IL-6, IL-8, MCP-1, RANTES and GM-CSF induced by pro-inflammatory stimuli. The MG262-mediated inhibition of pro-inflammatory cytokine production involves the inactivation of NF-κB. In conclusion, non-cytotoxic treatment with MG262 reduces the proliferative, fibrotic, and inflammatory response of nasal fibroblasts, whereas high MG262 concentrations induce apoptosis. The current study provides evidence of the effect of a proteasome inhibitor and its action mechanisms in a human *in vitro* cell culture model. Caution is required, however, before proposing proteasome inhibition as an alternative therapeutic strategy for reducing inflammation and fibro-proliferation in airway inflammatory diseases such as chronic asthma or nasal polyposis. In this respect, the anti-fibrotic and anti-inflammatory effects of proteasome inhibitors should be demonstrated in other cell types and, more importantly, proteasome inhibitors should be tested *in vivo* in animal models of the disease, with especial attention to the apoptotic-inducing effects of these drugs.

Acknowledgments

We thank Isabel Crespo and Cristina López (Plataforma de Citometria i Separació Cel·lular, CEK, IDIBAPS), and Maria Calvo and Anna Bosch (Unitat de Microscòpia Confocal-Serveis Cientificotècnics, Facultat de Medicina, Universitat de Barcelona, IDIBAPS) for their assistance in the cytometry and immunocytochemistry protocols. We also thank Marta Bosch (Departament de Biologia Cel·lular i Patologia, Facultat de Medicina, Universitat de Barcelona) for her assistance in the apoptosis studies.

Authorship Contributions

Participated in research design: Pujols, Agell, Mullol, and Picado.

Conducted experiments: Pujols, Fernández-Bertolín, Fuentes-Prado, and Roca-Ferrer.

Sample collection and clinical data acquisition: Alobid.

Performed data analysis and interpretation: Pujols, Roca-Ferrer, and Agell.

Wrote or contributed to the writing of the manuscript: Pujols, Agell, Mullol, and Picado.

REFERENCES

Adams J (2003) The proteasome: structure, function, and role in the cell. *Cancer Treatment Rev* **29:** 3-9.

Bachert C, Van Bruaene N, Toskala E, Zhang N, Olze H, Scadding G, Van Drunen CM, Mullol J, Cardell L, Gevaert P, Van Zele T, Claeys S, Halldén C, Kostamo K, Foerster U, Kowalski M, Bieniek K, Olszewska-Ziaber A, Nizankowska-Mogilnicka E, Szczeklik A, Swierczynska M, Arcimowicz M, Lund V, Fokkens W, Zuberbier T, Akdis C, Canonica G, Van Cauwenberge P, Burney P, and Bousquet J (2009) Important research questions in allergy and related diseases: 3-chronic rhinosinusitis and nasal polyposis - a GA^{2}LEN study. *Allergy* **64:** 520-533.

Barnes PJ and Karin M (1997) Nuclear factor-kappaB: a pivotal transcription factor in chronic inflammatory diseases. *N Engl J Med* **336:** 1066-1071.

Burgess JK (2009) The role of the extracellular matrix and specific growth factors in the regulation of inflammation and remodelling in asthma. *Pharmacol Ther* **122:** 19-29.

Carmignac V, Quéré R, and Durbeej M (2011) Proteasome inhibition improves the muscle of laminin α2 chain-deficient mice. *Hum Mol Genet* **20:** 541-552.

Codony-Servat J, Tapia MA, Bosch M, Oliva C, Domingo-Domenech J, Mellado B, Rolfe M, Ross JS, Gascon P, Rovira A, and Albanell J (2006) Differential cellular and molecular effects of bortezomib, a proteasome inhibitor, in human breast cancer cells. *Mol Cancer Ther* **5:** 665-675.

Cuschieri J, Gourlay D, Garcia I, Jelacic S, and Maier RV (2004) Implications of proteasome inhibition: an enhanced macrophage phenotype. *Cell Immunol* **227:** 140-147.

Domingo-Domènech J, Pippa R, Tápia M, Gascón P, Bachs O, and Bosch M (2008) Inactivation of NF-kappaB by proteasome inhibition contributes to increased apoptosis

induced by histone deacetylase inhibitors in human breast cancer cells. *Breast Cancer Res Treat* **112:** 53-62.

Elliott PJ, Pien CS, McCormack TA, Chapman ID, and Adams J (1999) Proteasome inhibition: A novel mechanism to combat asthma. *J Allergy Clin Immunol* **104:** 294-300.

Elmore S (2007) Apoptosis: a review of programmed cell death. *Toxicol Pathol* **35:** 495-516.

Fineschi S, Bongiovanni M, Donati Y, Djaafar S, Naso F, Goffin L, Argiroffo CB, Pache JC, Dayer JM, Ferrari-Lacraz S, and Chizzolini C (2008) In vivo investigations on anti-fibrotic potential of proteasome inhibition in lung and skin fibrosis. *Am J Respir Cell Mol Biol* **39:** 458-465.

Fineschi S, Reith W, Guerne PA, Dayer JM, and Chizzolini C (2006) Proteasome blockade exerts an antifibrotic activity by coordinately down-regulating type I collagen and tissue inhibitor of metalloproteinase-1 and up-regulating metalloproteinase-1 production in human dermal fibroblasts. *FASEB J* **20:** 562-564.

Fokkens W, Lund V, Mullol J; European Position Paper on Rhinosinusitis and Nasal Polyps group (2007) European position paper on rhinosinusitis and nasal polyps 2007. *Rhinol Suppl* **20:** 1-136.

Gerber A, Heimburg A, Reisenauer A, Wille A, Welte T, and Bühling F (2004) Proteasome inhibitors modulate chemokine production in lung epithelial and monocytic cells. *Eur Respir J* **24:** 40-48.

Ghosh AK (2002) Factors involved in the regulation of type I collagen gene expression: implication in fibrosis. *Exp Biol Med* (Maywood) **227:** 301-314.

Ghosh AK, Bhattacharyya S, and Varga J (2004) The tumor suppressor p53 abrogates Smad-dependent collagen gene induction in mesenchymal cells. *J Biol Chem* **279:** 47455-47463.

Ghosh AK, Bhattacharyya S, Wei J, Kim S, Barak Y, Mori Y, and Varga J (2009) Peroxisome proliferator-activated receptor-gamma abrogates Smad-dependent collagen stimulation by targeting the p300 transcriptional coactivator. *FASEB J* **23:** 2968-2977.

Goffin L, Seguin-Estévez Q, Alvarez M, Reith W, and Chizzolini C (2010) Transcriptional regulation of matrix metalloproteinase-1 and collagen 1A2 explains the anti-fibrotic effect exerted by proteasome inhibition in human dermal fibroblasts. *Arthritis Res Ther* **12:** R73.

Goldbaum O, Vollmer G, and Richter-Landsberg C (2006) Proteasome inhibition by MG-132 induces apoptotic cell death and mitochondrial dysfunction in cultured rat brain oligodendrocytes but not in astrocytes. *Glia* **53:** 891-901.

Goulet S, Bihl MP, Gambazzi F, Tamm M, and Roth M (2007) Opposite effect of corticosteroids and long-acting beta(2)-agonists on serum- and TGF-beta(1)-induced extracellular matrix deposition by primary human lung fibroblasts. *J Cell Physiol* **210:** 167-176.

Guo Y, Yang K, Harwalkar J, Nye JM, Mason DR, Garrett MD, Hitomi M, and Stacey DW (2005) Phosphorylation of cyclin D1 at Thr 286 during S phase leads to its proteasomal degradation and allows efficient DNA synthesis. *Oncogene* **24:** 2599-2612.

Hideshima T, Mitsiades C, Akiyama M, Hayashi T, Chauhan D, Richardson P, Schlossman R, Podar K, Munshi NC, Mitsiades N, and Anderson KC (2003) Molecular mechanisms mediating antimyeloma activity of proteasome inhibitor PS-341. *Blood* **101:** 1530-1534.

Hideshima T, Richardson P, Chauhan D, Palombella VJ, Elliott PJ, Adams J, and Anderson KC (2001) The proteasome inhibitor PS-341 inhibits growth, induces apoptosis, and overcomes drug resistance in human multiple myeloma cells. *Cancer Res* **61:** 3071-3076.

Hipp MS, Urbich C, Mayer P, Wischhusen J, Weller M, Kracht M, and Spyridopoulos I (2002) Proteasome inhibition leads to NF-kappaB-independent IL-8 transactivation in human endothelial cells through induction of AP-1. *Eur J Immunol* **32:** 2208-2217.

Kawakami A, Nakashima T, Sakai H, Hida A, Urayama S, Yamasaki S, Nakamura H, Ida H, Ichinose Y, Aoyagi T, Furuichi I, Nakashima M, Migita K, Kawabe Y, and Eguchi K (1999) Regulation of synovial cell apoptosis by proteasome inhibitor. *Arthritis Rheum* **42:** 2440-2448.

Le Bellego F, Perera H, Plante S, Chakir J, Hamid Q, and Ludwig MS (2009) Mechanical strain increases cytokine and chemokine production in bronchial fibroblasts from asthmatic patients. *Allergy* **64:** 32-39.

Ling YH, Liebes L, Jiang JD, Holland JF, Elliott PJ, Adams J, Muggia FM, and Perez-Soler R (2003a) Mechanisms of proteasome inhibitor PS-341-induced G(2)-M-phase arrest and apoptosis in human non-small cell lung cancer cell lines. *Clin Cancer Res* **9:** 1145-1154.

Ling YH, Liebes L, Zou Y, and Perez-Soler R (2003b) Reactive oxygen species generation and mitochondrial dysfunction in the apoptotic response to Bortezomib, a novel proteasome inhibitor, in human H460 non-small cell lung cancer cells. *J Biol Chem* **278:** 33714-33723.

Liu Y, Shepherd EG, and Nelin LD (2007) MAPK phosphatases--regulating the immune response. *Nat Rev Immunol* **7:** 202-212.

Ludwig A, Fechner M, Wilck N, Meiners S, Grimbo N, Baumann G, Stangl V, and Stangl K (2009) Potent anti-inflammatory effects of low-dose proteasome inhibition in the vascular system. *J Mol Med* **87:** 793-802.

Meiners S, Hocher B, Weller A, Laule M, Stangl V, Guenther C, Godes M, Mrozikiewicz A, Baumann G, and Stangl K (2004) Downregulation of matrix metalloproteinases and collagens and suppression of cardiac fibrosis by inhibition of the proteasome. *Hypertension* **44:** 471-477.

Meiners S, Ludwig A, Stangl V, and Stangl K (2008) Proteasome inhibitors: poisons and remedies. *Med Res Rev* **28:** 309-327.

Meyer JE, Berner I, Teran LM, Bartels J, Sticherling M, Schröder JM, and Maune S (1998) RANTES production by cytokine-stimulated nasal fibroblasts: its inhibition by glucocorticoids. *Int Arch Allergy Immunol* **117:** 60-67.

Moutzouris JP, Che W, Ramsay EE, Manetsch M, Alkhouri H, Bjorkman AM, Schuster F, Ge Q, and Ammit AJ (2010) Proteasomal inhibition upregulates the endogenous MAPK deactivator MKP-1 in human airway smooth muscle: mechanism of action and effect on cytokine secretion. *Biochim Biophys Acta* **1803:** 416-423.

Mutlu GM, Budinger GR, Wu M, Lam AP, Zirk A, Rivera S, Urich D, Chiarella SE, Go LH, Ghosh AK, Selman M, Pardo A, Varga J, Kamp DW, Chandel NS, Sznajder JI, and Jain M (2012) Proteasomal inhibition after injury prevents fibrosis by modulating TGF-beta1 signalling. *Thorax* **67:** 139-146.

Myllyharju J and Kivirikko KI (2004) Collagens, modifying enzymes and their mutations in humans, flies and worms. *Trends Genet* **20:** 33-43.

Nacu N, Luzina IG, Highsmith K, Lockatell V, Pochetuhen K, Cooper ZA, Gillmeister MP, Todd NW, and Atamas SP (2008) Macrophages produce TGF-beta-induced (beta-ig-h3) following ingestion of apoptotic cells and regulate MMP14 levels and collagen turnover in fibroblasts. *J Immunol* **180:** 5036-5044.

Nonaka M, Pawankar R, Saji F, and Yagi T (1999) Distinct expression of RANTES and GM-CSF by lipopolysaccharide in human nasal fibroblasts but not in other airway fibroblasts. *Int Arch Allergy Immunol* **119:** 314-321.

Ortiz-Lazareno PC, Hernandez-Flores G, Dominguez-Rodriguez JR, Lerma-Diaz JM, Jave-Suarez LF, Aguilar-Lemarroy A, Gomez-Contreras PC, Scott-Algara D, and Bravo-Cuellar A (2008) MG132 proteasome inhibitor modulates proinflammatory cytokines production and expression of their receptors in U937 cells: involvement of nuclear factor-kappaB and activator protein-1. *Immunology* **124:** 534-541.

Palombella VJ, Conner EM, Fuseler JW, Destree A, Davis JM, Laroux FS, Wolf RE, Huang J, Brand S, Elliott PJ, Lazarus D, McCormack T, Parent L, Stein R, Adams J, and Grisham MB (1998) Role of the proteasome and NF-kappaB in streptococcal cell wall-induced polyarthritis. *Proc Natl Acad Sci USA* **95:** 15671-15676.

Pawliczak R, Lewandowska-Polak A, and Kowalski ML (2005) Pathogenesis of nasal polyps: an update. *Curr Allergy Asthma Rep* **5:** 463-471.

Pfaffl MW (2001) A new mathematical model for relative quantification in real-time RT–PCR. *Nucleic Acids Res* **29:** e45.

Poznic M (2009) Retinoblastoma protein: a central processing unit. *J Biosci* **34:** 305-312.

Pujols L, Fuentes-Prado M, Fernández-Bertolín L, Alobid I, Roca-Ferrer J, Mullol J, and Picado C (2011) Lower sensitivity of nasal polyp fibroblasts to glucocorticoid anti-proliferative effects. *Respir Med* **105:** 218-225.

Schmidt N, Gonzalez E, Visekruna A, Kühl AA, Loddenkemper C, Mollenkopf H, Kaufmann SH, Steinhoff U, and Joeris T (2010) Targeting the proteasome: partial inhibition of the proteasome by bortezomib or deletion of the immunosubunit LMP7 attenuates experimental colitis. *Gut* **59:** 896-906.

Sherr CJ and Roberts JM (1999) CDK inhibitors: positive and negative regulators of G1-phase progression. *Genes & Dev* **13:** 1501-1512.

Silbiger S, Lei J, and Neugarten J (1999) Estradiol suppresses type I collagen synthesis in mesangial cells via activation of activator protein-1. *Kidney Int* **55:** 1268-1276.

Small GW, Shi YY, Edmund NA, Somasundaram S, Moore DT, and Orlowski RZ (2004) Evidence that mitogen-activated protein kinase phosphatase-1 induction by proteasome inhibitors plays an antiapoptotic role. *Mol Pharmacol* **66:** 1478-1490.

Small GW, Shi YY, Higgins LS, and Orlowski RZ (2007) Mitogen-activated protein kinase phosphatase-1 is a mediator of breast cancer chemoresistance. *Cancer Res* **67:** 4459-4466.

Xing Z, Jordana M, Braciak T, Ohtoshi T, and Gauldie J (1993) Lipopolysaccharide induces expression of granulocyte/macrophage colony-stimulating factor, interleukin-8, and interleukin-6 in human nasal, but not lung, fibroblasts: evidence for heterogeneity within the respiratory tract. *Am J Respir Cell Mol Biol* **9:** 255-263.

Wang J and Maldonado MA (2006) The ubiquitin-proteasome system and its role in inflammatory and autoimmune diseases. *Cell Mol Immunol* **3:** 255-261.

Yang Y, Ikezoe T, Saito T, Kobayashi M, Koeffler HP, and Taguchi H (2004) Proteasome inhibitor PS-341 induces growth arrest and apoptosis of non-small cell lung cancer cells via the JNK/c-Jun/AP-1 signaling. *Cancer Sci* **95:** 176-180.

Yannaki E, Papadopoulou A, Athanasiou E, Kaloyannidis P, Paraskeva A, Bougiouklis D, Palladas P, Yiangou M, and Anagnostopoulos A (2010) The proteasome inhibitor bortezomib drastically affects inflammation and bone disease in adjuvant-induced arthritis in rats. *Arthritis Rheum* **62:** 3277-3288.

You BR and Park WH (2011) Proteasome inhibition by MG132 induces growth inhibition and death of human pulmonary fibroblast cells in a caspase-independent manner. *Oncol Rep* **25:** 1705-1712.

FOOTNOTES

J.M. and C.P. contributed equally to this work, with senior responsibilities. This work was supported by grants from Fondo de Investigación Sanitaria [PI050057], Fundació La Marató de TV3 [MTV3-040630] and FUCAP-Beca Maria Ravà 2008. The research activity of L.P. is supported by Instituto de Salud Carlos III - Fondo de Investigación Sanitaria [050149].

This work was previously presented in part as follows: Pujols L, Fuentes M, Fernández-Bertolín L, Alobid I, Agell N, Roca-Ferrer J, Mullol J, and Picado C (2009). Effects of the reversible proteasome inhibitor MG262 on fibroblast proliferation and function, at the 7th EAACI-GA^{2}LEN Immunology Winter School; 5-8 February 2009, Davos, Switzerland.

Address correspondence to: Laura Pujols, Institut d'Investigacions Biomèdiques August Pi i Sunyer (IDIBAPS), lab 402, Hospital Clínic, Villarroel 170, 08036, Barcelona, Spain. E-mail: lpujols@clinic.ub.es

FIGURE LEGENDS

Figure 1. Effect of MG262 on nasal fibroblast viability. Nasal mucosa (*continuous lines*) and nasal polyp (*dashed lines*) fibroblasts were incubated with DMEM supplemented with 0.5% FBS with/without the simultaneous addition of MG262 for (**A**) 24 h, (**B**) 48 h, or (**C**) 72 h, or with bortezomib for 48 h (**D**). Cell viability was then determined by measuring (490 nm) the formation of a soluble formazan salt by metabolic active (viable) cells using the XTT assay. Data represent the median and interquartile range of at least *n*= 5 independent experiments from different patients. *p< 0.05 vs untreated cells.

Figure 2. Effect of MG262 on nasal fibroblast apoptosis. (**A**) Fibroblasts were incubated with DMEM supplemented with 0.5% FBS with or without z-VAD-FMK (50 μM) for 1 h prior to MG262 exposure for 48 h. Cell viability was measured by the XTT assay as indicated in Figure 1. *p< 0.01 vs 0% FBS; †p< 0.001 vs 0.5% FBS; #p< 0,01 vs z-VAD-FMK. (**B**) Fibroblasts were incubated with 0.5% FBS-supplemented DMEM with/without the simultaneous addition of MG262 for 24 h. Cells were then incubated with the fluorescent mitochondrial dye $DiOC_6$ (40 nM), stained with a violet-fluorescent reactive dye (Live/Dead fixable dead cell stain kit) and the percentages of viable cells exhibiting loss of mitochondrial membrane potential ($\Delta\Psi m$) determined by FACS. *p< 0.05 compared to untreated (C) cells. Graphs **A** and **B** show the median (bars) and interquartile range (whiskers) of *n*= 5 independent experiments from different patients. (**C**) Fibroblasts were incubated with 0.5% FBS-supplemented DMEM with/without the simultaneous addition of MG262 for 24 and 48 h. Cellular lysates were then obtained, electrophoresed on SDS-polyacrylamide gels, transferred to nitrocellulose membranes, and membranes incubated with primary antibodies against cleaved caspase-3, PARP and β-actin. Images are representative Western blots of *n*= 3 independent experiments from different patients.

Figure 3. Involvement of c-Jun in MG262-mediated nasal fibroblast cell death. (**A**) Fibroblasts were incubated with DMEM supplemented with 5% FBS with/without the simultaneous addition of MG262 for 6 and 24 h. Cellular lysates were then obtained, electrophoresed on SDS-polyacrylamide gels, transferred to nitrocellulose membranes, and membranes incubated with primary antibodies. Images are representative Western blots of phosphorylated c-Jun, total c-Jun, MKP-1 and β-actin. The 42 kDa band detected in MKP-1 Western blots is a non-specific band, supposedly, MKP-2. (**B**) Quantification of p-c-Jun and MKP-1 Western blots of the time-course experiments with MG262 shown in **A**. **$p<0.01$ and ***$p<0.001$ vs 5% FBS. (**C-E**) Fibroblasts were transfected with 20 nM of c-Jun siRNA or a negative control siRNA using lipofectamine RNAiMAX, as indicated in Materials and Methods. Forty-eight hours after transfection, cells were incubated with MG262 (10 nM) for 48 h. (**C**) Cellular lysates of adhered cells were then obtained and analyzed for the immunodetection of p-c-Jun and β-actin by Western blot. (**D**) The viability of c-Jun or negative control siRNA-transfected fibroblasts was measured by the XTT assay as indicated in Figure 1; *$p<0.05$. (**E**) The cell culture supernatants of the experiments shown in **C** were collected and the number of dead cells counted by the Trypan-blue dye exclusion method; *$p<0.05$. Results shown in **A** and **B** and **C** to **E** are derived from $n= 7$ and $n= 4$ independent experiments from different patients, respectively. All graphs show the median (bar) and interquartile range (whiskers).

Figure 4. Effect of MG262 on nasal fibroblast cell cycle. (**A**) Fibroblasts were treated with cell medium supplemented with 5% FBS with/without the simultaneous addition of MG262 (10 nM) for 24 h. Cells were then fixed/permeabilized in 70% ethanol and stained with propidium iodide, as indicated in Materials and Methods. DNA content was then measured by

FACS. Graphs show representative DNA profiles of 0% FBS-, 5% FBS- and MG262-treated fibroblasts. (**B**) Fibroblasts were treated with 5% FBS-supplemented medium with/without the simultaneous addition of MG262 (10 nM) for 22 h. Two hours before the end of this period the nucleoside 5-ethynyl-2´-deoxyuridine (EdU) was added to the cell cultures. Cells were then fixed in 70% ethanol, permeabilized with Triton X-100, and processed for the analysis of EdU incorporation into DNA by FACS, as indicated in Materials and Methods. Representative graphs of proliferating (Click-iT+) and non-proliferating cells of 0% FBS-, 5% FBS- and MG262-treated fibroblasts are shown. Data are representative of *n*= 6 (**A**) and *n*= 4 (**B**) independent experiments from different patients.

Figure 5. Effect of MG262 on cell cycle regulatory proteins in nasal fibroblasts. Fibroblasts were incubated with DMEM supplemented with 5% FBS with/without the simultaneous addition of MG262 (5, 10 and 50 nM) for different times (6 and 24 h). Cellular lysates were then obtained, electrophoresed on SDS-polyacrylamide gels, transferred to nitrocellulose membranes, and membranes processed for the analysis of cell cycle regulatory proteins by Western Blot. (**A,B**) Representative images of phosphorylated and total retinoblastoma (Rb) proteins in (**A**) time-course and (**B**) concentration-response experiments with MG262. (**C**) Quantification of cyclin D1 after 6 and 24 h of MG262 exposure. *p<0.05. (**D,E**) Quantification of p21 (*upper graphs*) and p27 (*lower graphs*) in (**D**) time-course and (**E**) concentration-response experiments with MG262. Bars show the median and whiskers the interquartile range of *n*= 7 independent experiments from different patients. *p<0.05, **p<0.01 and ***p<0.001 vs 5% FBS.

Figure 6. Effect of MG262 on collagen mRNA expression in nasal fibroblasts. (**A,B**) Nasal mucosa and polyp fibroblasts were incubated with cell medium without FBS and MG262 for

1 h prior to either the addition (**A**) or not (**B**) of TGF-β (5 ng/ml) for 24 h. Total cellular RNA was then extracted and converted (1 μg) to cDNA, and the mRNA expression of collagens 1α1, 1α2 and 3α1 was analyzed by real-time PCR and normalized to the RNA polymerase II constitutive gene. Graphs show the median (bars) and interquartile range (whiskers) of (**A**) *n*= 7 (nasal mucosa) and *n*= 12 (nasal polyps) and (**B**) *n*= 5 independent experiments from different patients. *p<0.05, **p<0.01 and ***p<0.001 vs untreated; ††p<0.01 and †††p<0.001 vs TGF-β. (**C**) Fibroblasts were incubated with cell medium without FBS and MG262 (50 nM) for 1 h prior to the addition or not of TGF-β (5 ng/ml) for 24 h. Cellular lysates were then obtained, electrophoresed on SDS-polyacrylamide gels, transferred to nitrocellulose membranes, and membranes processed for the analysis of p-c-Jun, PPAR-γ, p53 and β-actin by Western Blot. Images are representative of *n*= 3 independent experiments from different patients.

Figure 7. Effect of MG262 on IL-6 and IL-8 production in nasal fibroblasts. (**A,B**) Nasal mucosa and polyp fibroblasts were incubated with cell medium supplemented with 10% csFBS in the absence or presence of (**A**) 5 to 500 nM of MG262, or (**B**) 10 μM of BMS-345541 (IKK/NF-κB inhibitor), 20 μM of SP600125 (JNK inhibitor), 10 μM of SB203580 (p38 MAPK inhibitor), 10 μM of U0126 (MEK1/2 inhibitor), or 1 μM of wortmannin (PI3K/Akt inhibitor) for 1 h prior to addition of IL-1β (10 ng/ml) for 4 h. IL-6 and IL-8 production in supernatants was measured by ELISA. Graphs show the median (bars) and interquartile range (whiskers) of *n*= 5 (**A**) and *n*= 3 (**B**) independent experiments from different patients. **p<0.01 vs untreated; †p<0.05, ††p<0.01 and †††p<0.001 vs IL-β. (**C**) Fibroblasts were incubated with 10% csFBS-supplemented medium in the absence or presence of MG262 (500 nM) for 1 h prior to IL-1β stimulation (100 ng/ml) for 30 min. Cells were then fixed, permeabilized, incubated with anti-p65 antibody and visualized by

fluorescence microscopy. Representative images of p65 immunocytochemistry from *n*= 3 independent experiments from different patients are shown. Bars, 25 μm. (**D,E**) Fibroblasts were incubated in the absence or presence of MG262 (500 nM) as indicated in **C** and then stimulated with IL-1β (10 ng/ml) for (**D**) 5 to 15 min or (**E**) 4 h. Cellular lysates were obtained and processed for Western Blot analysis of p-IκBα, p-p38, p-c-Jun and β-actin. Images are representative of *n*= 2 (**D**) and *n*= 3 (**E**) independent experiments from different patients.

Figure 8. Effect of MG262 on the production of other pro-inflammatory mediators in nasal fibroblasts. Nasal mucosa and polyp fibroblasts were incubated with 10% csFBS-supplemented medium in the absence or presence of 50 and 500 nM of MG262 for 1 h prior to addition of IL-1β (10 ng/ml) for 4 h. MCP-1, RANTES and GM-CSF production in supernatants was measured with Cytometric Bead Array Flex Sets by FACS. Graphs show the median (bars) and interquartile range (whiskers) of *n*= 5 independent experiments from different patients. *$p<0.05$ and **$p<0.01$ vs untreated; †$p<0.05$ and ††$p<0.01$ vs IL-β.

TABLES

Table 1. Effect of MG262 on the cell cycle and DNA replication of nasal fibroblasts.

Cell treatment	G0/1 phase (n= 6)	S phase (n= 6)	G2/M phase (n= 6)	DNA replicating cells (n= 4)
0% FBS	92 (88.7-94.8)	1.9 (1.1-4.2)	5.3 (3.4-7.1)	4.7 (0.8-7.7)
5% FBS	65.3 (50.2-76.8)**	13.3 (8.6-16.6)**	19.2 (13.8-34.3)*	25.8 (17.8-37.8)**
MG262 (10 nM)	91.9 (86.5-95.3)†	2.1 (1-3.8)†	4.8 (2.6-8.1)††	0.5 (0.2-2.6)†††

Results expressed as median and interquartile range (%). *p< 0.05 and **p< 0.01 vs 0% FBS-treated cells; †p< 0.05, ††p< 0.01, and †††p<0.001 vs 5% FBS-treated cells.

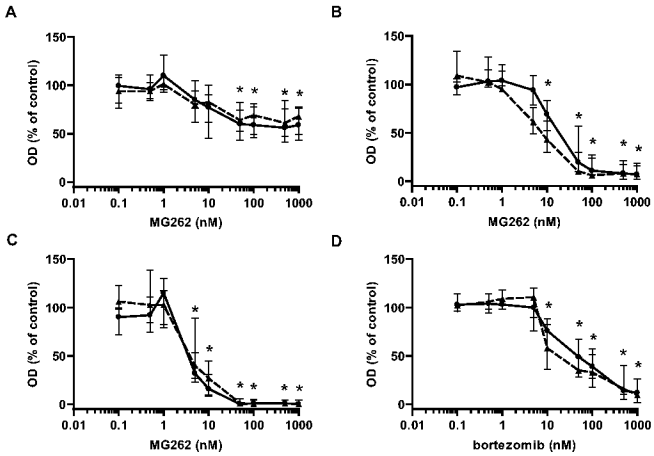
A
B
C
D
OD (% of control)
150
100
50
0
0.01
0.1
1
10
100
1000
MG262 (nM)
bortezomib (nM)
*

Figure 1_R1

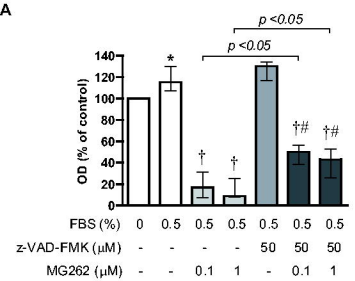
A
p <0.05
p <0.05
OD (% of control)
140
120
100
80
60
40
20
0
*
†
†
†#
†#
FBS (%) 0 0.5 0.5 0.5 0.5 0.5 0.5
z-VAD-FMK (μM) - - - - 50 50 50
MG262 (μM) - - 0.1 1 - 0.1 1

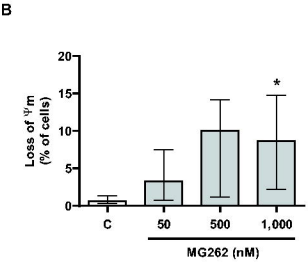
B
Loss of ψm (% of cells)
20
15
10
5
0
*
C
50
500
1,000
MG262 (nM)

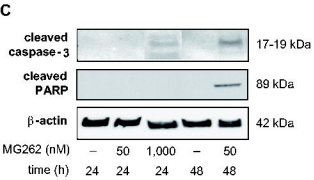
C
cleaved caspase-3
17-19 kDa
cleaved PARP
89 kDa
β-actin
42 kDa
MG262 (nM) – 50 1,000 – 50
time (h) 24 24 24 48 48

Figure 2_R1

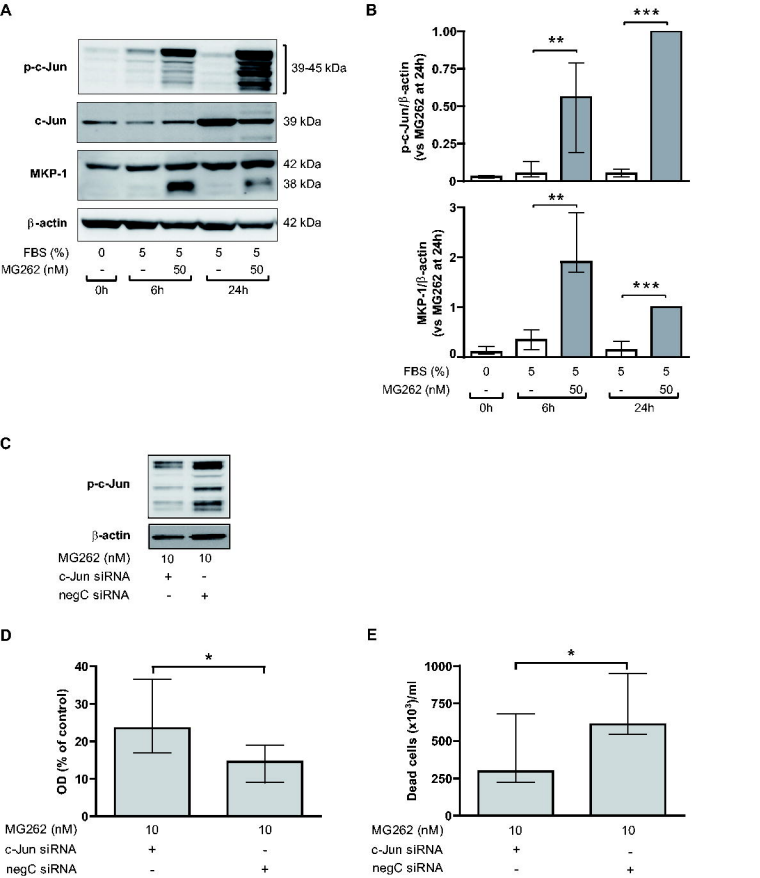
A
p-c-Jun
39-45 kDa
c-Jun
39 kDa
MKP-1
42 kDa
38 kDa
β-actin
42 kDa
FBS (%) 0 5 5 5 5
MG262 (nM) - - 50 - 50
0h 6h 24h
B
p-c-Jun/β-actin (vs MG262 at 24h)
1.00
0.75
0.50
0.25
0
**
***
MKP-1/β-actin (vs MG262 at 24h)
3
2
1
0
**
***
FBS (%) 0 5 5 5 5
MG262 (nM) - - 50 - 50
0h 6h 24h
C
p-c-Jun
β-actin
MG262 (nM) 10 10
c-Jun siRNA + -
negC siRNA - +
D
OD (% of control)
40
30
20
10
0
*
MG262 (nM) 10 10
c-Jun siRNA + -
negC siRNA - +
E
Dead cells (x10³)/ml
1000
750
500
250
0
*
MG262 (nM) 10 10
c-Jun siRNA + -
negC siRNA - +

Figure 3_R1

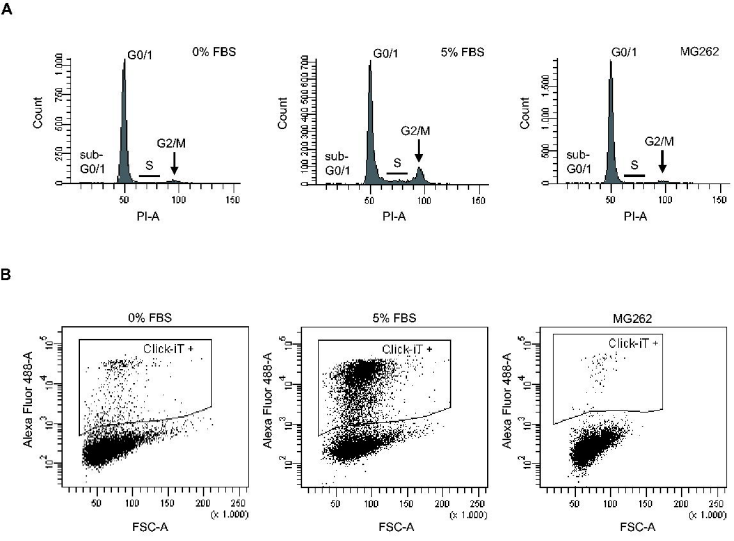
A
G0/1
0% FBS
sub-
G0/1
S
G2/M
Count
PI-A
G0/1
5% FBS
sub-
G0/1
S
G2/M
Count
PI-A
G0/1
MG262
sub-
G0/1
S
G2/M
Count
PI-A
B
0% FBS
Click-IT +
Alexa Fluor 488-A
FSC-A
(x 1.000)
5% FBS
Click-IT +
Alexa Fluor 488-A
FSC-A
(x 1.000)
MG262
Click-IT +
Alexa Fluor 488-A
FSC-A
(x 1.000)

Figure 4_R1

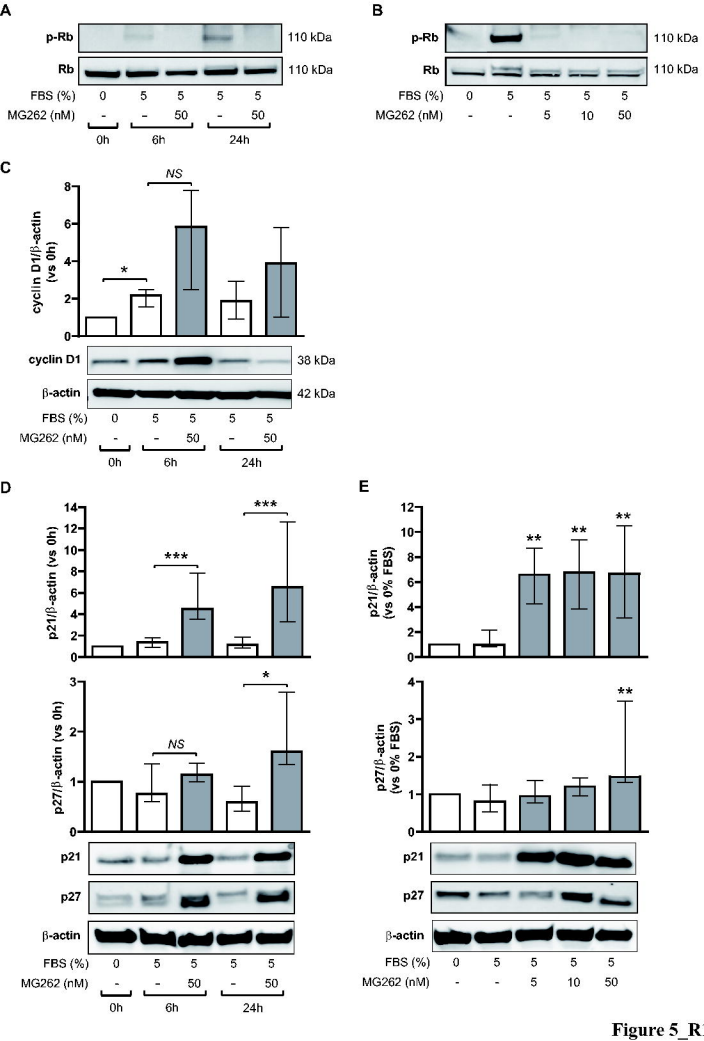
A
p-Rb
110 kDa
Rb
110 kDa
FBS (%) 0 5 5 5 5
MG262 (nM) - - 50 - 50
0h 6h 24h
B
p-Rb
110 kDa
Rb
110 kDa
FBS (%) 0 5 5 5 5
MG262 (nM) - - 5 10 50
C
cyclin D1/β-actin (vs 0h)
NS
*
cyclin D1
38 kDa
β-actin
42 kDa
FBS (%) 0 5 5 5 5
MG262 (nM) - - 50 - 50
0h 6h 24h
D
p21/β-actin (vs 0h)
***
***
p27/β-actin (vs 0h)
NS
*
p21
p27
β-actin
FBS (%) 0 5 5 5 5
MG262 (nM) - - 50 - 50
0h 6h 24h
E
p21/β-actin (vs 0% FBS)
**
**
**
p27/β-actin (vs 0% FBS)
**
p21
p27
β-actin
FBS (%) 0 5 5 5 5
MG262 (nM) - - 5 10 50

Figure 5_R1

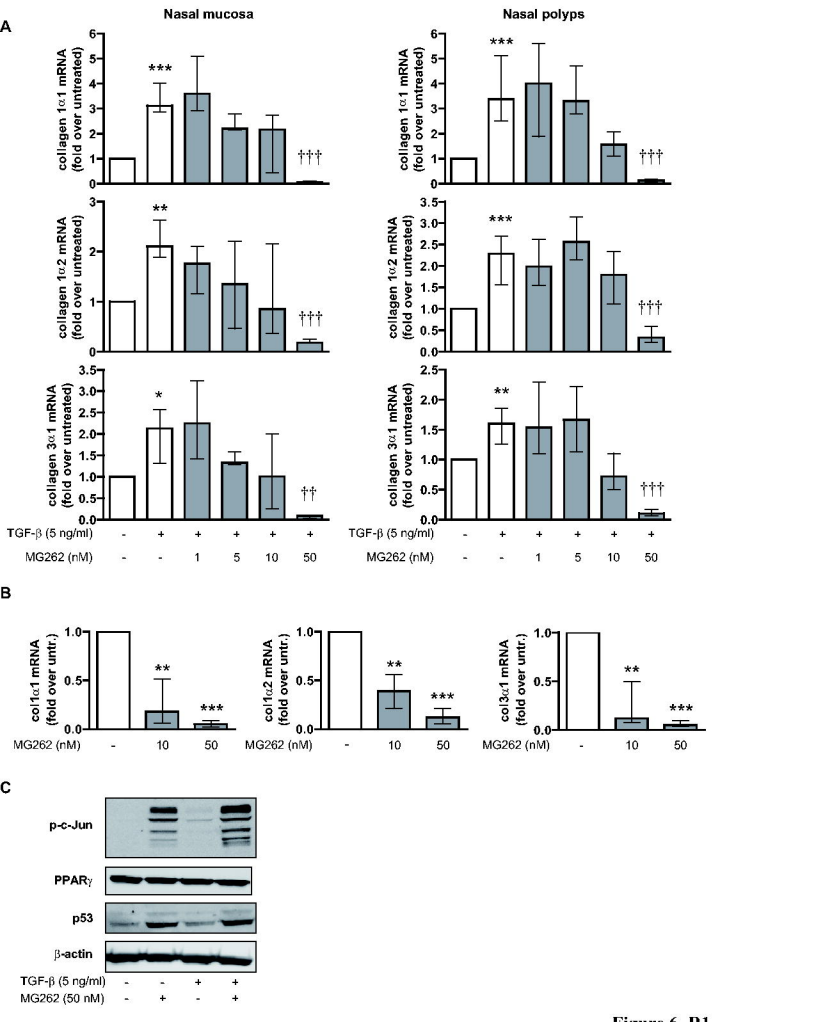
A
Nasal mucosa
Nasal polyps
collagen 1α1 mRNA (fold over untreated)
collagen 1α2 mRNA (fold over untreated)
collagen 3α1 mRNA (fold over untreated)
***
**
*
†††
††
TGF-β (5 ng/ml) - + + + + +
MG262 (nM) - - 1 5 10 50
B
col1α1 mRNA (fold over untr.)
col1α2 mRNA (fold over untr.)
col3α1 mRNA (fold over untr.)
MG262 (nM) - 10 50
C
p-c-Jun
PPARγ
p53
β-actin
TGF-β (5 ng/ml) - - + +
MG262 (50 nM) - + - +

Figure 6_R1

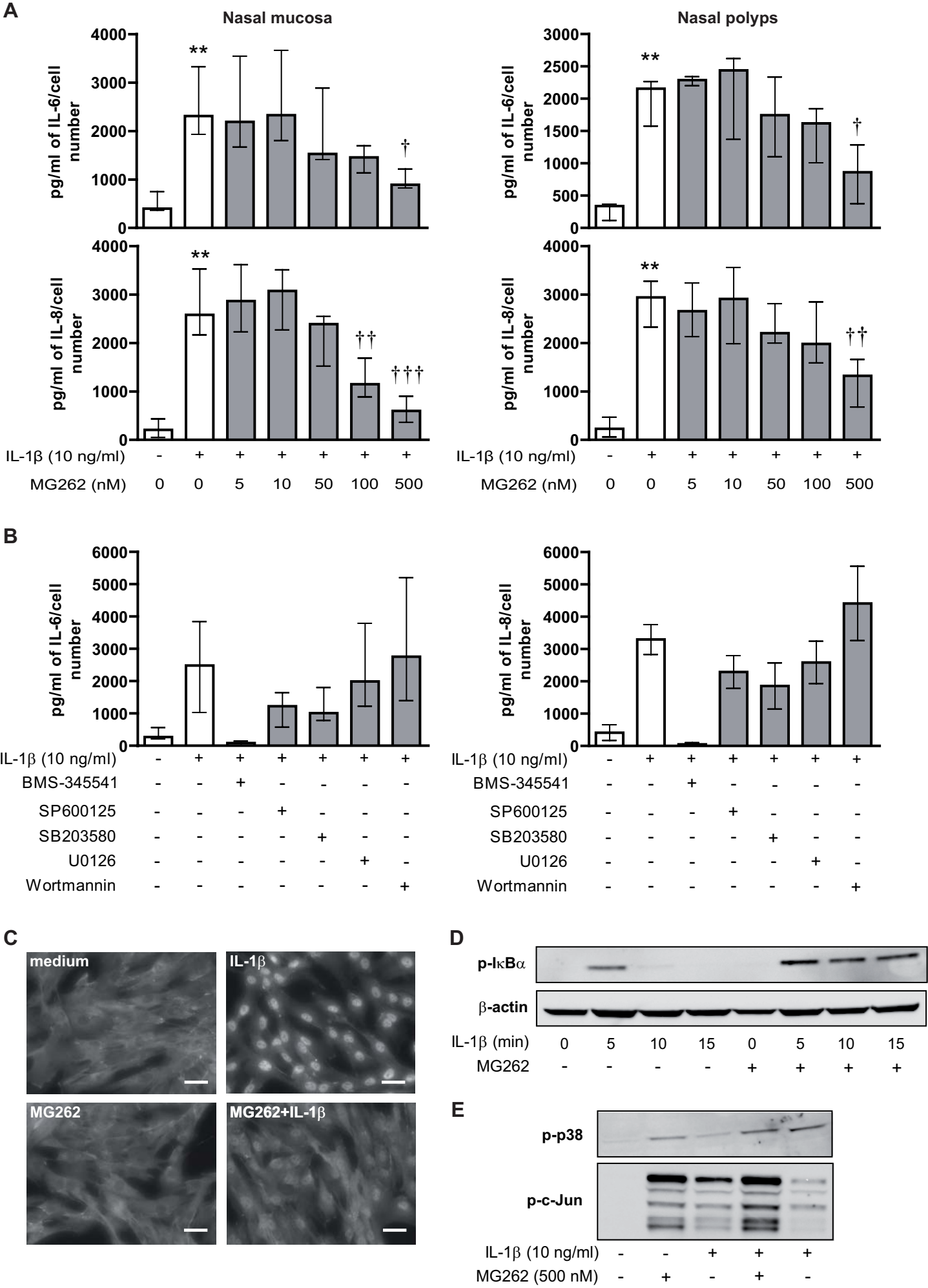
A
Nasal mucosa
Nasal polyps
pg/ml of IL-6/cell number
pg/ml of IL-8/cell number
IL-1β (10 ng/ml)
MG262 (nM)
B
BMS-345541
SP600125
SB203580
U0126
Wortmannin
C
medium
IL-1β
MG262
MG262+IL-1β
D
p-IκBα
β-actin
IL-1β (min)
MG262
E
p-p38
p-c-Jun
IL-1β (10 ng/ml)
MG262 (500 nM)

Figure 7_R1

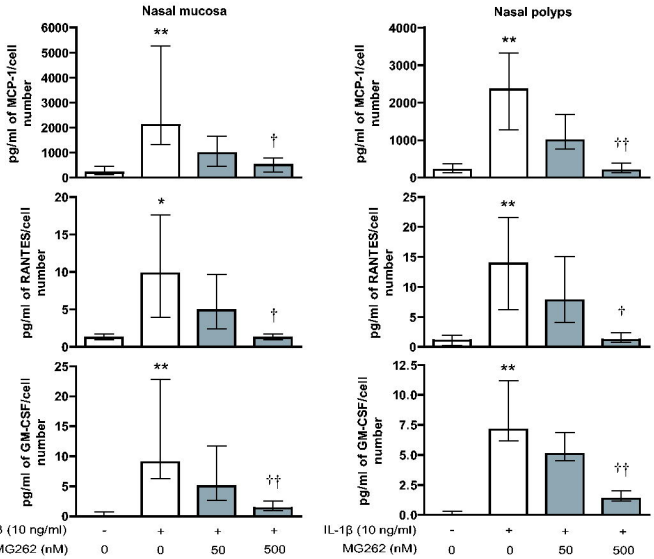
Nasal mucosa
Nasal polyps
pg/ml of MCP-1/cell number
pg/ml of RANTES/cell number
pg/ml of GM-CSF/cell number
IL-1β (10 ng/ml)
MG262 (nM)
0
50
500

Figure 8_R1